

# Lattice QCD calculation of $\pi\pi$ scattering length

Ziwen Fu

Key Laboratory of Radiation Physics and Technology (Sichuan University), Ministry of Education;  
Institute of Nuclear Science and Technology, Sichuan University, Chengdu 610064, P. R. China.

We study  $s$ -wave pion-pion ( $\pi\pi$ ) scattering length in lattice QCD for pion masses ranging from 330 MeV to 466 MeV. In the “Asqtad” improved staggered fermion formulation, we calculate the  $\pi\pi$  four-point functions for isospin  $I = 0$  and 2 channels, and use chiral perturbation theory at next-to-leading order to extrapolate our simulation results. Extrapolating to the physical pion mass gives the scattering lengths as  $m_\pi a_0^{I=2} = -0.0416(2)$  and  $m_\pi a_0^{I=0} = 0.186(2)$  for isospin  $I = 2$  and 0 channels, respectively. Our lattice simulation for  $\pi\pi$  scattering length in the  $I = 0$  channel is an exploratory study, where we include the disconnected contribution, and our preliminary result is near to its experimental value. These simulations are performed with MILC 2 + 1 flavor gauge configurations at lattice spacing  $a \approx 0.15$  fm.

PACS numbers: 12.38.Gc, 13.75.Lb, 11.15.Ha

## I. INTRODUCTION

Pion-pion scattering at low energies is elemental and important hadron-hadron scattering process. The  $s$ -wave  $\pi\pi$  scattering lengths are predicted at leading order (LO) in chiral perturbation theory ( $\chi$ PT) by Weinberg [1] in terms of pion mass,  $m_\pi$ , and pion decay constant,  $f_\pi$ , as

$$m_\pi a_{\pi\pi}^{I=0} \approx \frac{7m_\pi^2}{16\pi f_\pi^2} = 0.160; \quad m_\pi a_{\pi\pi}^{I=2} \approx -\frac{m_\pi^2}{8\pi f_\pi^2} = -0.0456.$$

The next-to-leading order (NLO) corrections depend on unknown low energy constants, which can be obtained from experimental measurements or lattice QCD.

The recent measurements of the  $K_{e4}$  decays [2] and  $K^\pm \rightarrow \pi^\pm \pi^0 \pi^0$  decays [3] by NA48/2 at CERN [4] give,  $m_\pi a_{\pi\pi}^{I=0} = 0.221(5)$  and  $m_\pi a_{\pi\pi}^{I=2} = -0.0429(47)$ . Including  $\chi$ PT constraints in their analysis, the determination of  $s$ -wave  $\pi\pi$  scattering lengths reaches [5, 6]:

$$m_\pi a_{\pi\pi}^{I=0} = 0.220(5); \quad m_\pi a_{\pi\pi}^{I=2} = -0.0444(10). \quad (1)$$

Lattice calculations of  $\pi\pi$  scattering have been studied in quenched QCD by various groups [7–12], and first full QCD calculation of  $\pi\pi$  scattering length was done to study isospin  $I = 2$   $s$ -wave scattering [13]. First fully-dynamical calculation of  $I = 2$   $\pi\pi$  scattering length was performed by NPLQCD [14, 15]. Mixed-action  $\chi$ PT at NLO was used to perform the chiral and continuum extrapolations, and obtain

$$m_\pi a_{\pi\pi}^{I=2} = -0.04330(42) \quad \text{and} \quad l_{\pi\pi}^{I=2}(\mu) = 6.2 \pm 1.2,$$

where  $l_{\pi\pi}^{I=2}(\mu)$  is a low energy constant (LEC), which is evaluated at physical pion decay constant  $f_{\pi,\text{phy}}$ . Using the  $N_f = 2$  maximally twisted mass fermion ensembles, Xu Feng et al [16] adopt the lightest pion mass, perform an explicit check for large lattice artifacts, and find

$$m_\pi l_{\pi\pi}^{I=2} = -0.04385(28), \quad l_{\pi\pi}^{I=2}(\mu = f_{\pi,\text{phy}}) = 4.65(85),$$

which is in agreement with the above experimental measurements and phenomenological analysis.

So far, only few efforts have been taken for  $I = 0$  case. Using the quenched approximation Y. Kuramashi et al. explored the  $I = 0$  channel, but the disconnect diagram was neglected for some reasons [8]. Qi Liu performed full QCD calculation for the  $I = 0$  channel with the consideration of disconnected graph, however the scattering length has a large error, and serves only as a bound on the magnitude [17].

It is well-known that  $I = 0$  channel is a great challenging phenomenologically because of  $\sigma$  resonance. Encouraged by our trustful measurement of  $\pi K$  scattering [18], here we use MILC gauge configurations generated with 2 + 1 flavors of Asqtad improved staggered dynamical sea quarks [19] to investigate  $s$ -wave  $\pi\pi$  scattering for  $I = 0$  and 2 channels. We measure all the diagrams with extra efforts to the disconnect diagram. We note an attractive signal for the  $I = 0$  channel and repulsive one in the  $I = 2$  case. As presented later, after chiral extrapolation, we find at the physical pion mass

$$m_\pi a_{\pi\pi}^{I=0} = 0.186(2); \quad m_\pi a_{\pi\pi}^{I=2} = -0.0416(2),$$

which is in reasonable agreement with above experimental measurements and phenomenological analysis as well as previous lattice calculations. Moreover, we perform an exploratory work for calculating  $l_{\pi\pi}^{I=0}(\mu)$ , which is a LEC appearing in  $\chi$ PT description of the quark mass dependence of the scattering length for the  $I = 0$  channel.

## II. METHOD

Let us study the scattering of two Nambu-Goldstone pions in the Asqtad-improved staggered dynamical fermion formalism at zero momentum. Here we follow the original conventions and notations in Refs. [7, 8, 10]. Using operators  $O_\pi(x_1)$ ,  $O_\pi(x_2)$  for pions at points  $x_1$  and  $x_2$ , respectively, we then express the  $\pi\pi$  four-point functions as

$$C_{\pi\pi}(x_4, x_3, x_2, x_1) = \langle O_\pi(x_4) O_\pi(x_3) O_\pi^\dagger(x_2) O_\pi^\dagger(x_1) \rangle,$$

where  $\langle \dots \rangle$  stands for the expectation value of path integral. After summing over the spatial coordinates, we achieve  $\pi\pi$  four-point function in zero-momentum state,

$$C_{\pi\pi}(t_4, t_3, t_2, t_1) = \sum_{\mathbf{x}_1} \sum_{\mathbf{x}_2} \sum_{\mathbf{x}_3} \sum_{\mathbf{x}_4} C_{\pi\pi}(x_4, x_3, x_2, x_1),$$

where  $x_1 \equiv (\mathbf{x}_1, t_1)$ ,  $x_2 \equiv (\mathbf{x}_2, t_2)$ ,  $x_3 \equiv (\mathbf{x}_3, t_3)$ ,  $x_4 \equiv (\mathbf{x}_4, t_4)$ , and  $t$  represents time difference, i.e.,  $t \equiv t_3 - t_1$ . We choose  $t_1 = 0, t_2 = 1, t_3 = t$ , and  $t_4 = t + 1$  to avert the Fierz rearrangement of the quark lines, and build  $\pi\pi$  operators for isospin  $I = 0$  and 2 eigenstates as

$$\begin{aligned} \mathcal{O}_{\pi\pi}^{I=0}(t) &= \frac{1}{\sqrt{3}} \left\{ \pi^-(t) \pi^+(t+1) + \pi^+(t) \pi^-(t+1) - \pi^0(t) \pi^0(t+1) \right\}, \\ \mathcal{O}_{\pi\pi}^{I=2}(t) &= \pi^+(t) \pi^+(t+1), \end{aligned} \quad (2)$$

with the pion interpolating field operators

$$\begin{aligned} \pi^+(t) &= - \sum_{\mathbf{x}} \bar{d}(\mathbf{x}, t) \gamma_5 u(\mathbf{x}, t), \\ \pi^-(t) &= \sum_{\mathbf{x}} \bar{u}(\mathbf{x}, t) \gamma_5 d(\mathbf{x}, t), \\ \pi^0(t) &= \frac{1}{\sqrt{2}} \sum_{\mathbf{x}} [\bar{u}(\mathbf{x}, t) \gamma_5 u(\mathbf{x}, t) - \bar{d}(\mathbf{x}, t) \gamma_5 d(\mathbf{x}, t)]. \end{aligned}$$

In the isospin limit, four diagrams contribute to  $\pi\pi$  scattering amplitudes [7, 8, 10]. The quark line diagrams contributing to  $\pi\pi$  four-point function are displayed in

Figure 1, and labeled as direct ( $D$ ), crossed ( $C$ ), rectangular ( $R$ ), and vacuum ( $V$ ) diagrams, respectively.

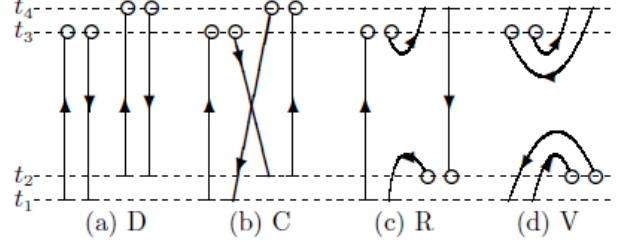


FIG. 1: Diagrams contributing to  $\pi\pi$  four-point functions. Short bars stand for wall sources. Open circles are sinks for local pion operator.

It is very difficult to reliably measure the rectangular ( $R$ ) and vacuum diagrams ( $V$ ) [8, 10]. In this work we use moving wall source method to solve it [8, 10, 18], namely, each propagator, which corresponds to a wall source at time slice  $t = 0, \dots, T - 1$ , are defined by

$$\sum_{n''} D_{n', n''} G_t(n'') = \sum_{\mathbf{x}} \delta_{n', (\mathbf{x}, t)}, \quad 0 \leq t \leq T - 1, \quad (3)$$

where  $D$  is the quark matrix. The combination of  $G_t(n)$  that we apply for  $\pi\pi$  four-point functions is schematically shown in Figure 1. and we can also express them in terms of the quark propagators  $G$ , namely,

$$\begin{aligned} C_{\pi\pi}^D(t_4, t_3, t_2, t_1) &= \sum_{\mathbf{x}_3} \sum_{\mathbf{x}_4} \langle \text{Re Tr}[G_{t_1}^\dagger(\mathbf{x}_3, t_3) G_{t_1}(\mathbf{x}_3, t_3) G_{t_2}^\dagger(\mathbf{x}_4, t_4) G_{t_2}(\mathbf{x}_4, t_4)] \rangle, \\ C_{\pi\pi}^C(t_4, t_3, t_2, t_1) &= \sum_{\mathbf{x}_3} \sum_{\mathbf{x}_4} \langle \text{Re Tr}[G_{t_1}^\dagger(\mathbf{x}_3, t_3) G_{t_2}(\mathbf{x}_3, t_3) G_{t_2}^\dagger(\mathbf{x}_4, t_4) G_{t_1}(\mathbf{x}_4, t_4)] \rangle, \\ C_{\pi\pi}^R(t_4, t_3, t_2, t_1) &= \sum_{\mathbf{x}_2} \sum_{\mathbf{x}_3} \langle \text{Re Tr}[G_{t_1}^\dagger(\mathbf{x}_2, t_2) G_{t_4}(\mathbf{x}_2, t_2) G_{t_4}^\dagger(\mathbf{x}_3, t_3) G_{t_1}(\mathbf{x}_3, t_3)] \rangle, \\ C_{\pi\pi}^V(t_4, t_3, t_2, t_1) &= \sum_{\mathbf{x}_2} \sum_{\mathbf{x}_3} \left\{ \text{Re} \langle \text{Tr}[G_{t_1}^\dagger(\mathbf{x}_2, t_2) G_{t_1}(\mathbf{x}_2, t_2)] \rangle \langle \text{Tr}[G_{t_4}^\dagger(\mathbf{x}_3, t_3) G_{t_4}(\mathbf{x}_3, t_3)] \rangle - \right. \\ &\quad \left. \text{Re} \langle \text{Tr}[G_{t_1}^\dagger(\mathbf{x}_2, t_2) G_{t_1}(\mathbf{x}_2, t_2)] \rangle \langle \text{Tr}[G_{t_4}^\dagger(\mathbf{x}_3, t_3) G_{t_4}(\mathbf{x}_3, t_3)] \rangle \right\}, \end{aligned} \quad (4)$$

where daggers is the conjugation by the even-odd parity  $(-1)^n$  for the Kogut-Susskind quark action. We utilize the hermiticity properties of the quark propagator  $G$  to remove the factors of  $\gamma^5$ . The vacuum diagram here is accompanied by a vacuum subtraction [20]. As it is discussed in Refs. [8, 10], the rectangular and vacuum diagrams create gauge-variant noise, which are suppressed by performing the gauge field average without gauge fixing [8, 10] in the current study.

All the four diagrams in Figure 1 can be combined to

build physical correlation functions for  $\pi\pi$  states with definite isospin. If we consider that  $u$  and  $d$  quarks have the same mass, the  $\pi\pi$  correlation function for  $I = 0$  and  $I = 2$  can be written in terms of these diagrams, namely,

$$\begin{aligned} C_{\pi\pi}^{I=0}(t) &\equiv \langle \mathcal{O}_{\pi\pi}^{I=0}(t) | \mathcal{O}_{\pi\pi}^{I=0}(0) \rangle \\ &= D + \frac{N_f}{2} C - 3N_f R + \frac{3}{2} V, \\ C_{\pi\pi}^{I=2}(t) &\equiv \langle \mathcal{O}_{\pi\pi}^{I=2}(t) | \mathcal{O}_{\pi\pi}^{I=2}(0) \rangle = D - N_f C, \end{aligned} \quad (5)$$

where  $N_f$  is inserted to address the flavor degrees of freedom of the Kogut-Susskind staggered fermion [7].

The  $s$ -wave  $\pi\pi$  scattering length in the continuum is defined by

$$a_0 = \lim_{k \rightarrow 0} \frac{\tan \delta_0(k)}{k}. \quad (6)$$

$k$  is the magnitude of the center-of-mass scattering momentum related to the total energy by  $E_{\pi\pi}^I = 2\sqrt{m_\pi^2 + k^2}$  of the  $\pi\pi$  system in a cubic box of size  $L$  with isospin  $I$ .  $\delta_0(k)$  is  $s$ -wave scattering phase shift, which can be calculated by the Lüscher's formula [22, 23],

$$\left(\frac{\tan \delta_0(k)}{k}\right)^{-1} = \frac{\sqrt{4\pi}}{\pi L} \cdot \mathcal{Z}_{00}\left(1, \frac{k^2}{(2\pi/L)^2}\right), \quad (7)$$

where the zeta function  $\mathcal{Z}_{00}(1; q^2)$  is defined by

$$\mathcal{Z}_{00}(1; q^2) = \frac{1}{\sqrt{4\pi}} \sum_{\mathbf{n} \in \mathbb{Z}^3} \frac{1}{n^2 - q^2}, \quad (8)$$

here  $q = kL/(2\pi)$ , and  $\mathcal{Z}_{00}(1; q^2)$  can be efficiently computed the method discussed in Refs. [13, 18].

The energy  $E_{\pi\pi}$  can be obtained from the  $\pi\pi$  four-point function denoted in Eq. (5) with the large  $t$ . At large  $t$  this correlator will fall as

$$C_{\pi\pi}^I(t) \propto e^{-E_{\pi\pi}t} + \dots, \quad (9)$$

where  $E_{\pi\pi}$  is the energy of the lightest two pion state. In the usual manner, pion mass  $m_\pi$  can be evaluated through

$$C_\pi(t) \propto e^{-m_\pi t} + \dots. \quad (10)$$

In our concrete calculation we evaluate the energy shift  $\delta E = E - 2m_\pi$  from the ratio

$$R^X(t) = \frac{C_{\pi\pi}^X(0, 1, t, t+1)}{C_\pi(0, t)C_\pi(1, t+1)}, \quad X = D, C, R, \text{ and } V,$$

where  $C_\pi(0, t)$  and  $C_\pi(1, t+1)$  are the pion two-point functions. The amplitudes which project out the  $I = 0$  and 2 isospin eigenstates can be written as

$$\begin{aligned} R_{I=0}(t) &= R^D(t) + \frac{N_f}{2} R^C(t) - 3N_f R^R(t) + \frac{3}{2} R^V(t), \\ R_{I=2}(t) &= R^D(t) - N_f R^C(t). \end{aligned} \quad (11)$$

We extract the energy shift  $\delta E$  from the ratio [7]

$$R_I(t) = Z_I e^{-\delta E t} + \dots, \quad (12)$$

where  $Z_I$  stands for wave function factor [8, 10].

### III. SIMULATION RESULTS

We use the MILC lattices in the presence of the 2 + 1 dynamical flavors of the Asqtad-improved staggered dynamical fermions, the description of its simulation parameters are given in Refs. [19, 24]. We analyzed the

$\pi\pi$  four-point functions on the 0.15 fm MILC ensemble of  $360 \times 16^3 \times 48$  gauge configurations with bare quark masses  $am_{ud}/am_s = 0.0097/0.0484$  and bare gauge coupling  $10/g^2 = 6.572$ , which has an inverse lattice spacing  $a^{-1} = 1.358^{+35}_{-12}$  GeV [19, 24]. The masses of the  $u$  and  $d$  quarks are degenerate.

We use the standard conjugate gradient method to obtain the required matrix element of the inverse fermion matrix. We compute the propagators on all the time slices  $t = 0, \dots, T-1$  of both source and sink. After averaging the correlators over all  $T = 48$  possible values, the statistics are significantly improved because we can place the pion source at all time slices.

With same configurations we compute the  $\pi\pi$  four point correlation functions using six  $u$  valence quarks, namely,  $am_x = 0.0097, 0.01067, 0.01261, 0.01358, 0.01455, \text{ and } 0.0194$ , where  $m_x$  is the light valence  $u$  quark mass.

In Figure 2 the individual ratios, which are defined in Eq. (11) corresponding to the diagrams in Figure 1,  $R^X$  ( $X = D, C, R$  and  $V$ ) are displayed as functions of  $t$  for  $am_x = 0.0097$ . It is extremely noisy for the disconnected diagram ( $V$ ), but still we can get a good signal up to time separation  $t = 14$ . Clear signals observed up to  $t = 19$  for the rectangular amplitude and up until  $t = 14$  for the vacuum amplitude demonstrate that the method of wall source without gauge fixing used here is practically applicable.

The values of the direct amplitude  $R^D$  is quite close to unity, indicating a weak interaction in this channel. The crossed amplitude, on the other hand, increases linearly up to  $t \sim 17$ , implying a repulsion in the  $I = 2$  channel. After a beginning increase up to  $t \sim 4$ , the rectangular amplitude shows a linear decrease up until  $t \sim 20$ , suggesting an attractive force between two pions. Moreover, the magnitude of this slope is analogous to that of the cross amplitude but with different sign. These characteristics are what we want [1, 7].

The vacuum amplitude is negligibly small up to  $t \sim 10 - 14$ , and loss of signals after that. This characteristic is in well accordance with the Okubo-Zweig-Iizuka (OZI) rule and  $\chi$ PT in leading order, which expects the disappearing of the vacuum amplitude [8]. Moreover, its the errors should be approximately independent of time separation  $t$ , and increases exponentially like  $e^{2m_\pi t}$  [8]. Therefore, it is very difficult to obtain its proper information from large time separation.

In Figure 3 we plot the ratio  $R_I(r)$  projected onto the isospin  $I = 0$  and 2 channels for  $am_x = 0.0097$ , which are denoted in Eq. (11). A decrease of the ratio of  $R_{I=2}(t)$  indicates a positive energy shift and hence a repulsive interaction for the  $I = 2$  channel, and an increase of  $R_{I=0}(t)$  suggests an attraction for the  $I = 0$  case. A dip at  $t = 3$  for the  $I = 0$  channel can be clearly noted [10].

In this work, we use Eq. (12) to extract the energy shift  $\delta E_I$ , and then insert them into the Eqs. (6) and (7) to obtain the scattering lengths. In this work, the energy shifts  $a\delta E$  are picked up from the effective energy shift

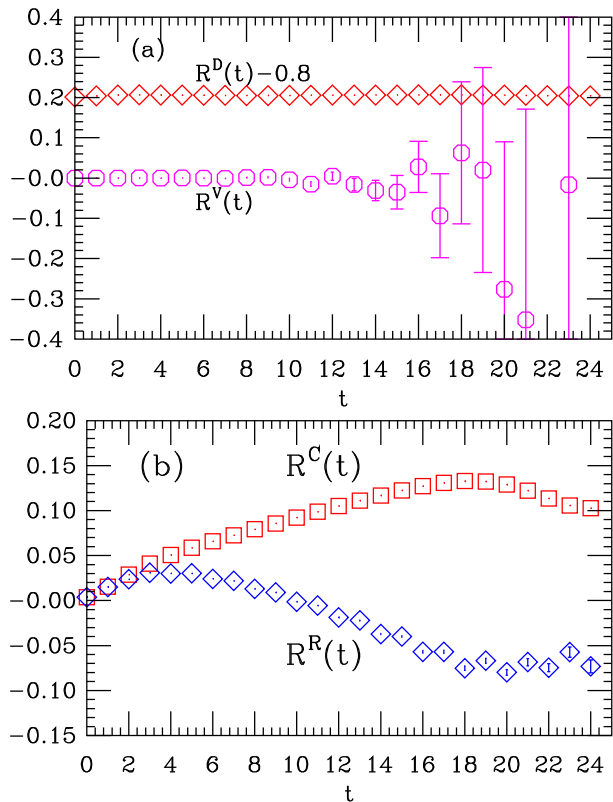


FIG. 2: Individual amplitude ratios  $R^X(t)$  as functions of  $t$ . (a) Direct diagram shifted by 0.8 (diamonds) and vacuum diagram (octagons); (b) crossed (squares) and rectangular (diamonds) diagrams.

plots, and they were selected by searching for a “plateau” in the energy shift as a function of the minimum distance  $D_{\min}$  as well as a good fit quality (namely,  $\chi^2$ ) [18].

We utilize the exponential physical fitting model in Eq. (12) to extract the desired energy shifts for both  $I = 2$  and 0 channels. In Figure 3 we display the ratio  $R_I(t)$  projected onto both channels for  $am_x = 0.0097$ . The fitted values of the energy shifts,  $\delta E_I$  in lattice units, fitting range, and wave function factor  $Z_I$  are summarized in Table I. The third block shows energy shifts in lattice units, Column four shows wave function factor  $Z_I$ , Column five shows time range for the chosen fit, and Column six shows degrees of freedom (dof) for the fit. The wave function  $Z_I$  factors are pretty close to unity and the  $\chi^2/\text{dof}$  is pretty small for the  $I = 2$  channel, indicating the values of the extracted scattering lengths are substantially reliable, and the  $Z$  factors are also near to unity, and the  $\chi^2/\text{dof}$  is reasonable for the  $I = 0$  channel, suggesting the value of the extracted scattering lengths are enough safe.

In our previous work [18, 25], we have measured the pion masses ( $m_\pi$ ) and the pion decay constants  $f_\pi$  [26], which are summarized in Table II. The second and third blocks show pion masses in lattice unit and in GeV, respectively, and Column four shows the pion decay con-

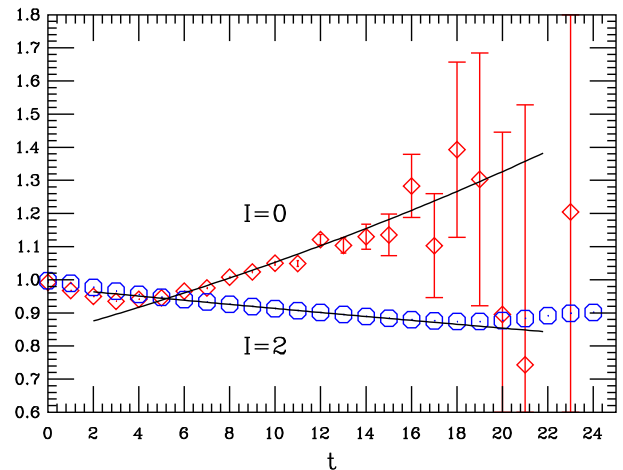


FIG. 3:  $R_I(t)$  for  $\pi\pi$  four-point function calculated without gauge fixing for  $am_x = 0.0097$ . Solid line in  $I = 2$  is exponential fits for  $10 \leq t \leq 15$  and Solid line in  $I = 0$  is exponential fits for  $7 \leq t \leq 14$ .

TABLE I: Summary of simulation results for energy shifts.

$I$	$m_x$	$\delta E$	$Z_I$	Range	$\chi^2/\text{dof}$
0	0.00970	-0.0241(19)	0.825(7)	7 – 14	12.8/6
	0.01067	-0.0235(32)	0.835(23)	7 – 14	9.46/6
	0.01261	-0.0222(29)	0.854(19)	6 – 12	6.94/5
	0.01358	-0.0223(30)	0.856(20)	6 – 12	5.33/5
	0.01455	-0.0217(32)	0.863(20)	6 – 10	4.66/3
2	0.01940	-0.0199(30)	0.884(19)	6 – 12	16.5/5
	0.00970	0.00670(15)	0.977(2)	10 – 15	1.07/4
	0.01067	0.00662(15)	0.980(2)	10 – 15	0.17/4
	0.01261	0.00648(14)	0.984(2)	10 – 15	0.05/4
	0.01358	0.00640(14)	0.986(2)	10 – 15	0.03/4
	0.01455	0.00625(13)	0.986(2)	10 – 15	0.02/4
	0.01940	0.00594(12)	0.993(2)	10 – 15	0.08/4

stants in lattice units. Now we can substitute these en-

TABLE II: Summary of the pion mass and the pion decay constants.

$m_x$	$am_\pi$	$m_\pi(\text{GeV})$	$af_\pi$
0.00970	0.2458(2)	0.334(6)	0.12136(29)
0.01067	0.2575(2)	0.350(6)	0.12264(34)
0.01261	0.2787(2)	0.379(7)	0.12425(27)
0.01358	0.2890(2)	0.392(7)	0.12482(32)
0.01455	0.2987(2)	0.406(7)	0.12600(26)
0.01940	0.3430(2)	0.466(8)	0.12979(27)

ergy shifts in Table I into the Eq. (6) to achieve the scattering lengths. The center-of-mass scattering momentum  $k^2$  in GeV calculated by  $E_{\pi K}^I = \delta E_I + 2m_\pi = 2\sqrt{m_\pi^2 + k^2}$  and then its  $s$ -wave scattering lengths  $a_0$  ob-

TABLE III: Summary of lattice simulation scattering lengths.

Isospin	$m_x$	$k^2$ [GeV]	$a_0$	$m_\pi a_0$
0	0.00970	-0.0107(4)	2.95(19)	0.724(48)
	0.01067	-0.0109(7)	3.03(32)	0.781(85)
	0.01261	-0.0112(7)	3.16(33)	0.882(92)
	0.01358	-0.0117(8)	3.40(38)	0.983(107)
	0.01455	-0.0118(8)	3.67(38)	1.095(112)
	0.01940	-0.0124(9)	3.78(50)	1.297(173)
2	0.00970	0.00306(7)	-0.495(5)	-0.121(2)
	0.01067	0.00316(7)	-0.509(5)	-0.131(1)
	0.01261	0.00335(7)	-0.537(5)	-0.150(1)
	0.01358	0.00343(7)	-0.548(5)	-0.159(2)
	0.01455	0.00345(7)	-0.552(5)	-0.165(2)
	0.01940	0.00378(8)	-0.598(6)	-0.205(2)

tained through Eq. (6) for both  $I = 0$ , and 2 channels are summarized in Table III. The errors come from the statistical errors of the fitted values of the energy shifts. The third block shows center-of-mass scattering momentum  $k^2$  in GeV, Column four shows  $s$ -wave scattering lengths in lattice units, and Column five shows pion mass times  $s$ -wave scattering lengths.

We adopt the formula predicted by  $\chi$ PT at NLO to extrapolate  $\pi\pi$  scattering lengths to the physical point. As suggested in Refs. [14–16], we carry out the chiral extrapolation of  $m_\pi a_{\pi\pi}^{I=2}$  and  $m_\pi a_{\pi\pi}^{I=0}$  in terms of  $m_\pi/f_\pi$  instead of  $m_\pi$ . Thus we use the continuum  $\chi$ PT forms of  $a_0^{I=2}$  and  $a_0^{I=0}$ , which are directly constructed from Appendix C in Ref. [27], as

$$m_\pi a_{\pi\pi}^{I=0} = \frac{7m_\pi^2}{16\pi f_\pi^2} \left\{ 1 - \frac{m_\pi^2}{16\pi^2 f_\pi^2} \left[ 9 \ln \frac{m_\pi^2}{f_\pi^2} - 5 - l_{\pi\pi}^{I=0}(\mu = f_{\pi,\text{phy}}) \right] \right\}, \quad (13)$$

$$m_\pi a_{\pi\pi}^{I=2} = -\frac{m_\pi^2}{8\pi f_\pi^2} \left\{ 1 + \frac{m_\pi^2}{16\pi^2 f_\pi^2} \left[ 3 \ln \frac{m_\pi^2}{f_\pi^2} - 1 - l_{\pi\pi}^{I=2}(\mu = f_{\pi,\text{phy}}) \right] \right\}, \quad (14)$$

where we plugged in the values of the pion mass  $m_\pi$ , and the pion decay constants  $f_\pi$ , which are summarized Table II, and  $l_{\pi\pi}^{I=0}(\mu)$  and  $l_{\pi\pi}^{I=2}(\mu)$  are related to the Gasser-Leutwyler coefficients  $\bar{l}_i$  as [27]

$$l_{\pi\pi}^{I=0}(\mu) = \frac{40}{21}\bar{l}_1 + \frac{80}{21}\bar{l}_2 - \frac{5}{7}\bar{l}_3 + 4\bar{l}_4 + 9 \ln \frac{m_{\pi,\text{phy}}^2}{\mu^2}, \quad (15)$$

$$l_{\pi\pi}^{I=2}(\mu) = \frac{8}{3}\bar{l}_1 + \frac{16}{3}\bar{l}_2 - \bar{l}_3 - 4\bar{l}_4 + 3 \ln \frac{m_{\pi,\text{phy}}^2}{\mu^2}, \quad (16)$$

here Eq. (16) were extensively used in Refs. [14–16].

The chiral extrapolation of  $\pi\pi$  scattering lengths,  $m_\pi a_0^{I=2}$  and  $m_\pi a_0^{I=0}$  are plotted by the dotted lines as a function of  $m_\pi^2$  in Figure 4. The fit parameters  $l_{\pi\pi}^{I=0}(\mu)$ ,  $l_{\pi\pi}^{I=2}(\mu)$ , and the  $s$ -wave scattering lengths  $m_\pi a_0$  at the physical points, where we adopt the latest PDG [28] values, are also summarized in Table IV. The chiral scale is taken as  $\mu = f_{\pi,\text{phy}}$ . From Figure 4, we can note that our lattice simulation results for the  $I = 2$  scattering length agrees well with the one-loop formula, while scattering length for  $I = 0$  have a large error, and is also in reasonable agreement with  $\chi$ PT at NLO.

TABLE IV: The fitted  $m_\pi a_0$  at the physical point.

Isospin	$\chi^2/\text{dof}$	$l_{\pi\pi}^I(\mu = f_{\pi,\text{phy}})$	$m_\pi a_0$
$I = 0$	0.268/5	$18.674 \pm 1.213$	0.186(2)
$I = 2$	9.864/5	$11.587 \pm 0.871$	-0.0416(2)

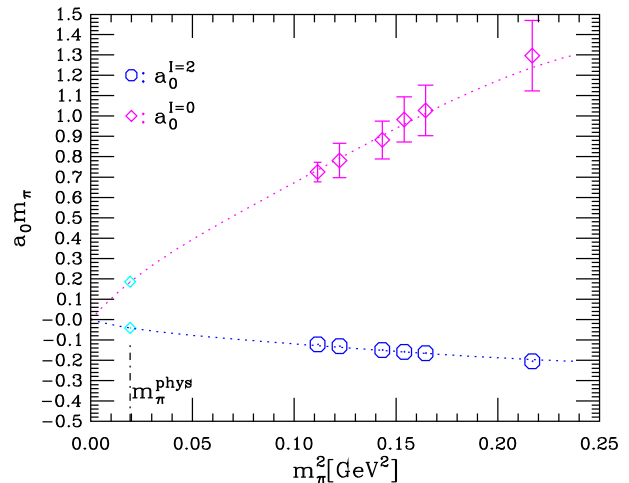


FIG. 4:  $m_\pi^2$ -dependence of  $\pi\pi$  scattering lengths  $m_\pi a_0$  for  $I = 0$  and 2 channels. The dotted lines give  $\chi$ PT predictions at NLO. The cyan diamond points indicate its physical values.

Although the fitted value of  $l_{\pi\pi}^{I=2}(\mu)$  is larger than that of other lattice studies [14–16], our fitted value of  $m_\pi a_{\pi\pi}^{I=2}$  is reasonable consistent with other lattice studies [14–16]. Since it is an exploratory study for  $I = 0$  channel, there are no lattice comparisons with our fitted values of  $l_{\pi\pi}^{I=0}(\mu)$  and  $m_\pi a_0$ . Anyway, our fitted value of  $s$ -wave  $\pi\pi$  scattering length for  $I = 0$  channel is in reasonable agreement with the experimental measurement

in Eq. (1).

#### IV. CONCLUSIONS AND OUTLOOKS

In this work, we performed a lattice study of  $s$ -wave  $\pi\pi$  scattering for isospin  $I = 0$  and 2 channels. We evaluated all of the four diagrams, and observed an attractive signal for the  $I = 0$  channel and a repulsive one for the  $I = 2$  channel, respectively. Extrapolating toward the physical point yields  $m_\pi a_0^{I=2} = -0.0416(2)$  and  $m_\pi a_0^{I=0} = 0.186(2)$  for  $I = 2$  and 0 channels, respectively, which are in good agreement with  $\chi$ PT at NLO, and  $m_\pi a_0^{I=2} = -0.0416(2)$  is reasonably consistent with other lattice studies [14–16]. Moreover, we give an exploratory fitted value of  $s$ -wave  $\pi\pi$  scattering length for  $I = 0$  channel, which is in reasonable agreement with the recent experimental measurement [4].

It is quite stimulating that  $\pi\pi$  scattering for the  $I = 0$

channel can be trustworthily calculated by wall sources without gauge fixing. It gives us hope that we can use this technique to tackle  $\sigma$  resonance, which is still poorly understood from lattice QCD.

In our previous works [25, 29, 30], we studied and evaluated  $\sigma$  mass, and found that the  $\sigma$  meson is heavier than the  $\pi\pi$  threshold for enough small  $u$  quark mass. These works as well as our lattice investigation for the  $\pi\pi$  scattering in the  $I = 0$  channel will stimulate people to investigate the decay mode  $\sigma \rightarrow \pi\pi$ .

Since our study is restricted only at zero momenta, it can not provide adequate information on  $\sigma$  meson. To investigate the  $\sigma$  resonance, we should study the  $\pi\pi$  scattering length at the  $I = 0$  channel with non-zero momentum, which is an indicative of a  $\sigma$  pole. We are beginning this kind of work, and the measurement of the  $\pi\pi$  scattering for the  $I = 0$  channel with the momentum  $p = (1, 0, 0)$  is in progress.

- 
- [1] S. Weinberg, Phys. Rev. Lett. **17** (1966) 616.
  - [2] J. R. Batley et al, Eur. Phys. J., C **54** (2008) 411.
  - [3] J. R. Batley et al, Eur. Phys. J., C **64** (2009) 589.
  - [4] Brigitte Bloch-Devaux, PoS, KAON09 (2009) 033.
  - [5] H. Leutwyler, arXiv:hep-ph/0612112.
  - [6] G. Colangelo, J. Gasser, and H. Leutwyler, Nucl. Phys., B **603** (2001) 125.
  - [7] S. R. Sharpe, R. Gupta and G. W. Kilcup, Nucl. Phys. B **383** (1992) 309.
  - [8] Y. Kuramashi et al, Phys. Rev. Lett. **71** (1993) 2387.
  - [9] M. Fukugita et al, Phys. Rev. Lett. **73** (1994) 2176.
  - [10] M. Fukugita et al, Phys. Rev. D **52** (1995) 3003.
  - [11] C. Liu, J. h. Zhang, Y. Chen and J. P. Ma, Nucl. Phys. B **624** (2002) 360.
  - [12] X. Li *et al.*, JHEP **0706** (2007) 053.
  - [13] T. Yamazaki et al, Phys. Rev. D **70** (2004) 074513.
  - [14] S. R. Beane, P. F. Bedaque, K. Orginos and M. J. Savage, Phys. Rev. D **73** (2006) 054503.
  - [15] Silas R. Beane et al, Phys. Rev., D **77** (2008) 014505.
  - [16] X. Feng, K. Jansen, D. B. Renner, Phys. Lett. B **684** (2010) 268.
  - [17] Q. Liu, PoS LAT2009 (2009) 101.
  - [18] Z. Fu, Phys. Rev. D **85**, 074501 (2012). arXiv:1110.1422 [hep-lat]
  - [19] C. Bernard et al, Phys. Rev. D **83** (2011) 034503.
  - [20] T. Blum et al, arXiv:1106.2714 [hep-lat].
  - [21] R. Gupta, G. Guralnik, G. W. Kilcup, S. R. Sharpe, Phys. Rev. D **43** (1991) 2003.
  - [22] M. Luscher, Nuclear Physics B **354** (1991) 531.
  - [23] L. Lellouch and M. Luscher, Commun. Math. Phys. **219** (2001) 31.
  - [24] A. Bazavov et al, Rev. Mod. Phys. **82** (2010) 1349.
  - [25] Z. Fu, Chin. Phys. Lett. **28** (2011) 081202.
  - [26] C. Aubin et al, Phys. Rev. D **70** (2004) 114501.
  - [27] J. Bijnens, G. Colangelo, G. Ecker, J. Gasser, and M. E. Sainio, Nucl. Phys., B **508** (1997) 263.
  - [28] Nakamura K et al, J. Phys. G **37** (2010) 075021.
  - [29] C. Bernard et al, Phys. Rev. D, **76** (2007) 094504
  - [30] Z. Fu and C. DeTar, Chin. Phys. C **35**(10) (2011) 896.